

## Supporting Information

### Construction of mesoporous S-doped $\text{Co}_3\text{O}_4$ with abundant oxygen vacancies as an efficient activator of PMS for organic dye degradation

Muxin Lu<sup>a,\*</sup>, Guiying Kang<sup>a</sup>, Yajuan Deng<sup>b</sup>

<sup>a</sup> College of Chemical Engineering and Technology, Tianshui Normal University, Tianshui, Gansu 741000, P. R. China

<sup>b</sup> Baoji Vocational & Technical College, Baoji, Shaanxi 721000, P. R. China

\* Corresponding author. E-mail address: lumuxin@tsnu.edu.cn (M.X. Lu).

#### Supplementary Text

##### 1. Characterisation

The  $\text{Co}_3\text{O}_4$  and S- $\text{Co}_3\text{O}_4$  samples were determined by X-ray powder diffraction (XRD) using Bruker D8 Advance X-ray diffractometer with Cu  $K\alpha$  radiation ( $\lambda = 1.5406 \text{ \AA}$ ). The morphology of sample was characterized by a Hitachi SU-8100 Field emission scanning electron microscope (SEM) equipped with an energy dispersive X-ray spectrometer (EDS). The nitrogen sorption isotherms of the products were obtained using a Micromeritics ASAP 2460 analyser operating at 77 K. The pore-size distribution derived from the adsorption branches of the isotherms was calculated based on the Nonlocal Density Functional Theory. The surface elemental composition and chemical state were analysed using X-ray photoelectron spectroscopy (XPS, Thermo Scientific NEXSA X-ray) as the reference C1s peak of the surface adventitious carbon. The electrochemical properties of the catalytic materials were

determined using an Ametek ModuLab XM multi-functional photoelectrochemical test system using  $\text{Na}_2\text{SO}_4$  solution ( $0.5 \text{ mol L}^{-1}$ ) as the supporting electrolyte. Inductively coupled plasma optical emission spectrometry (ICP-OES, Optima 8300, PerkinElmer) was employed to detect the relative contents of Co constituents. The active oxidative species were detected by Electron paramagnetic resonance (EPR) technique using a Bruker A300 spectrometer at ambient temperature.

### Supplementary Figures

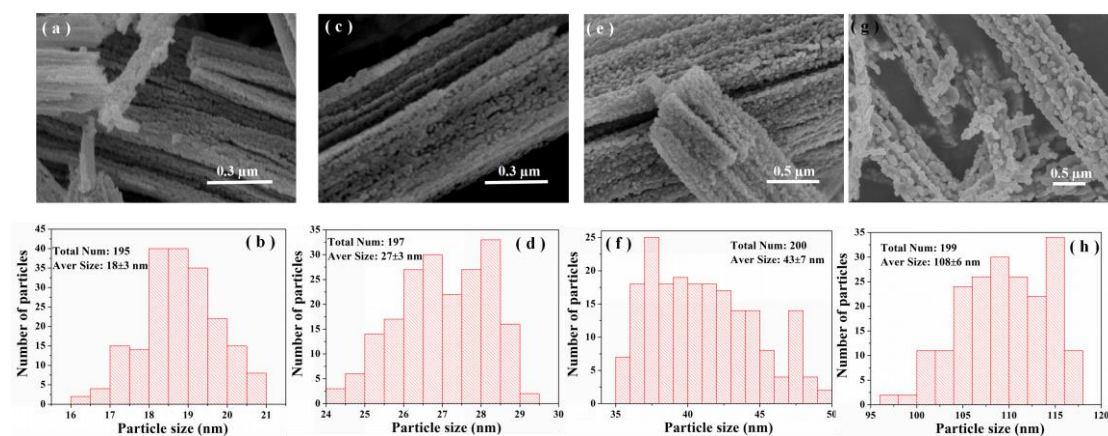


Fig. S1 SEM images and grain-size distributions of S-Co<sub>3</sub>O<sub>4</sub> calcined at different temperatures: (a, b) 350 °C, (c, d) 400 °C, (e, f) 450 °C and (g, h) 500 °C.

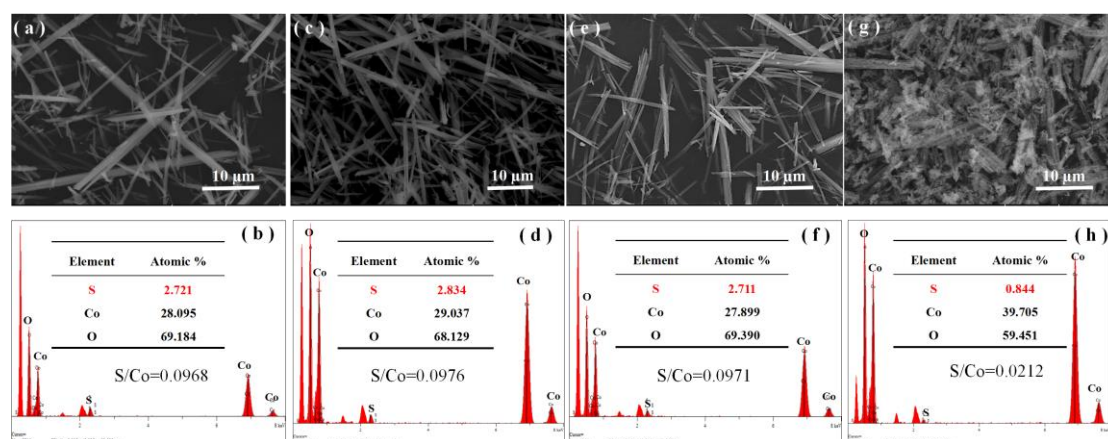


Fig. S2 SEM-EDS images of S-Co<sub>3</sub>O<sub>4</sub> calcined at different temperatures: (a, b) 350 °C, (c, d) 400 °C, (e, f) 450 °C and (g, h) 500 °C.

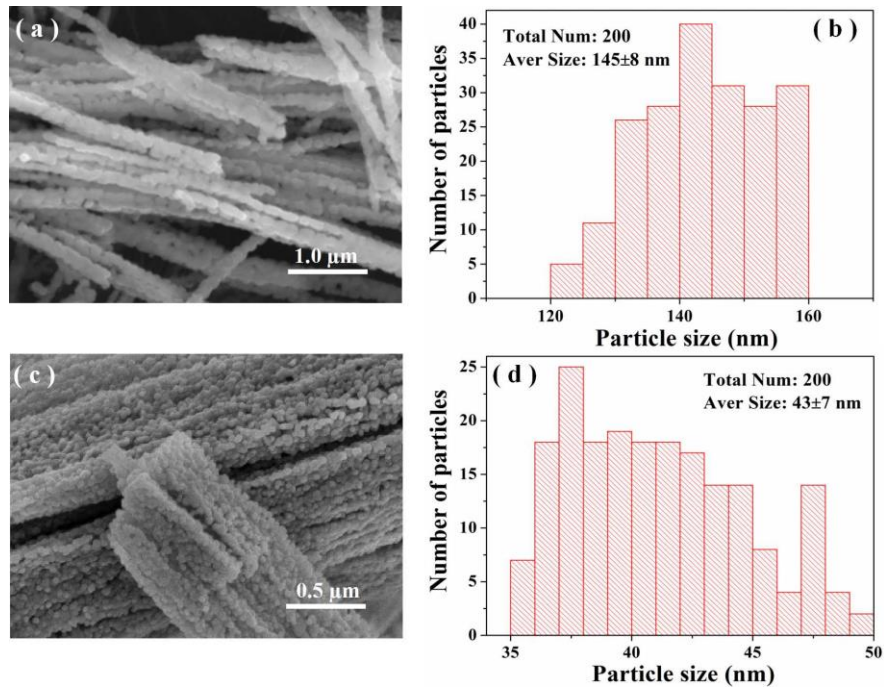


Fig. S3 SEM images and grain-size distributions of  $\text{Co}_3\text{O}_4$  (a, b) and  $\text{S-Co}_3\text{O}_4$  (c, d) calcined at 450 °C.

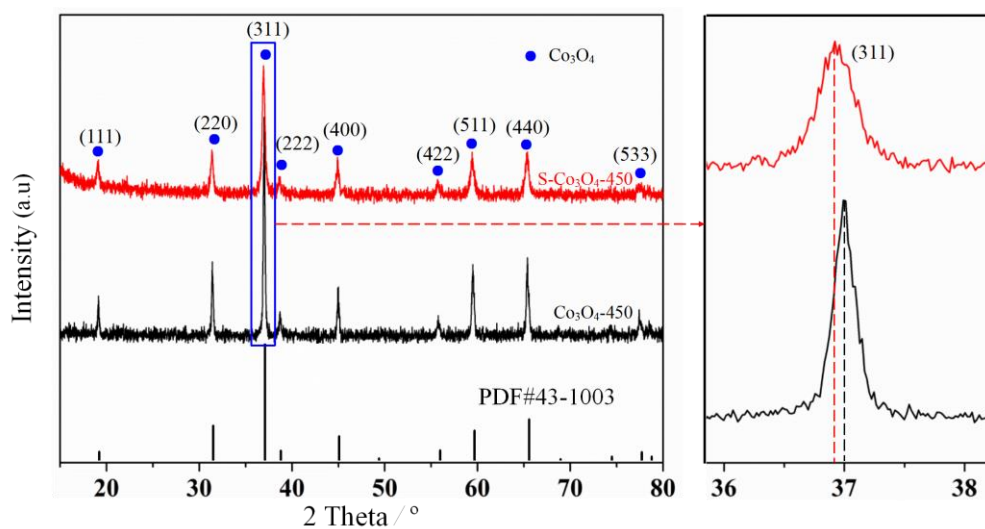


Fig. S4 XRD patterns of  $\text{Co}_3\text{O}_4$ -450 and  $\text{S-Co}_3\text{O}_4$ -450 samples.

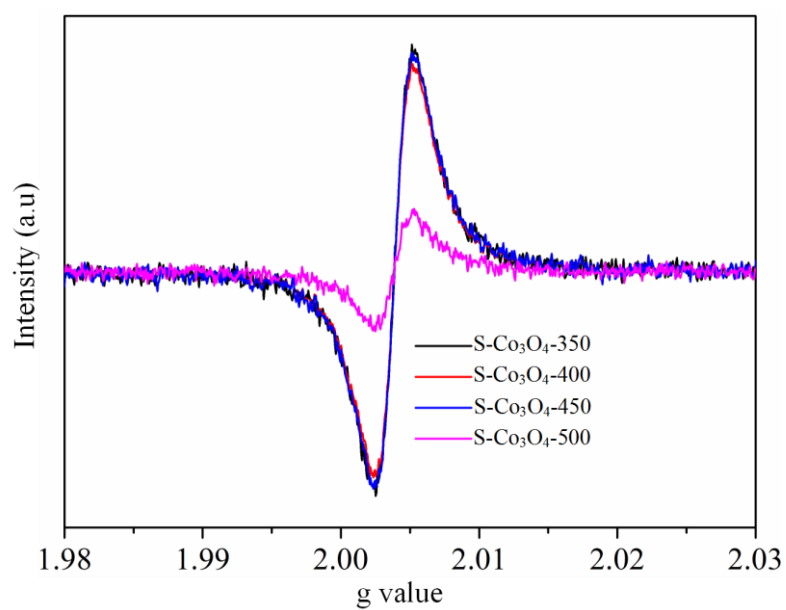


Fig. S5 EPR spectra of  $\text{S-Co}_3\text{O}_4$  calcined at different temperatures.

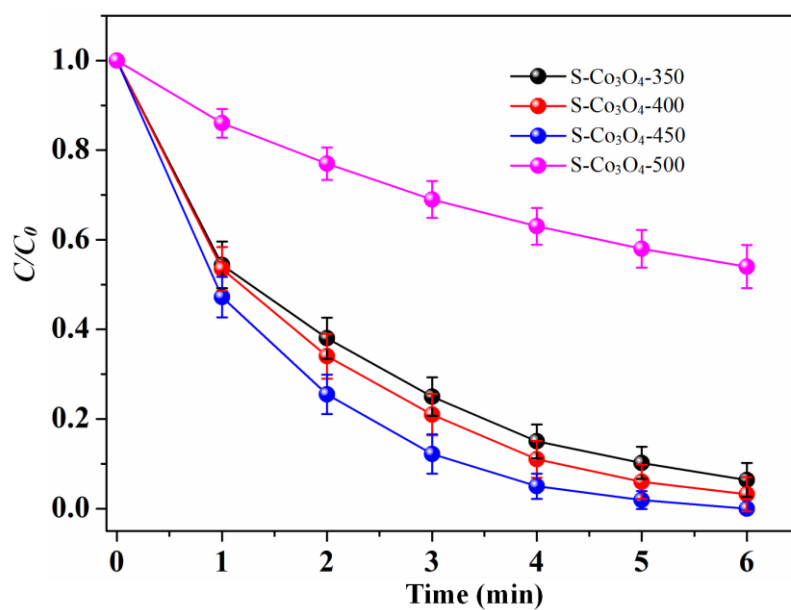


Fig. S6 Effect of S-Co<sub>3</sub>O<sub>4</sub> samples obtained at different calcination temperatures on the MB degradation rate.

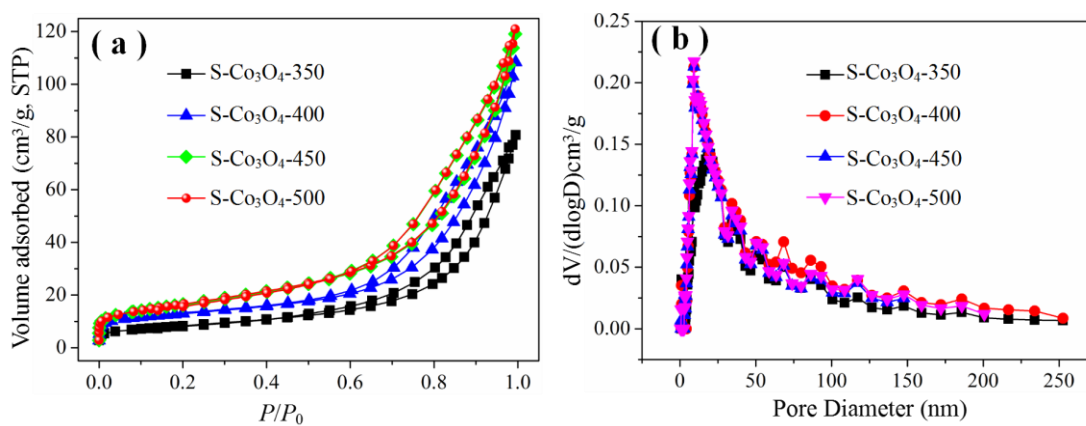


Fig. S7 N<sub>2</sub> adsorption and desorption isotherms (a) and pore diameter distributions (b) of S-Co<sub>3</sub>O<sub>4</sub> calcined at different temperatures.

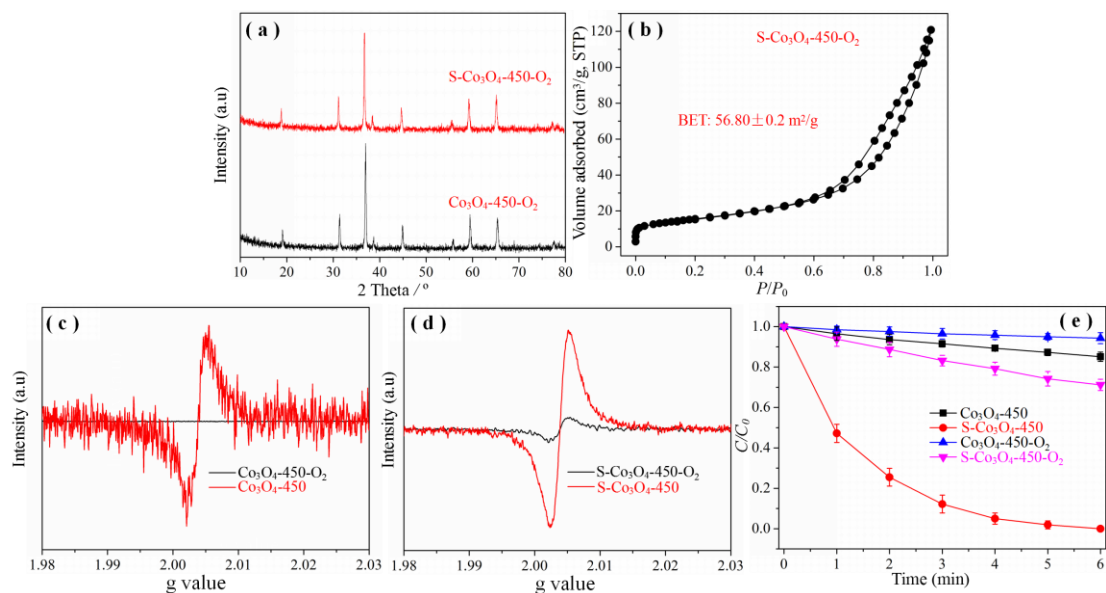


Fig S8 (a) XRD patterns of  $\text{Co}_3\text{O}_4\text{-450}$  and  $\text{S-Co}_3\text{O}_4\text{-450}$  after calcining at  $400^\circ\text{C}$  under an  $\text{O}_2$  atmosphere for 2 h; (b)  $\text{N}_2$  adsorption and desorption isotherms of  $\text{S-Co}_3\text{O}_4\text{-450}$  by calcining at  $400^\circ\text{C}$  under an  $\text{O}_2$  atmosphere for 2 h; EPR spectra of the  $\text{Co}_3\text{O}_4\text{-450}$  (c) and  $\text{S-Co}_3\text{O}_4\text{-450}$  (d) by calcining at  $400^\circ\text{C}$  under an  $\text{O}_2$  atmosphere for 2 h; (e) MB degradation rate in different samples activated PMS systems (conditions:  $T = 25^\circ\text{C}$ ,  $[\text{MB}] = 20 \text{ mg/L}$ ,  $[\text{PMS}] = 0.1 \text{ g/L}$ ,  $[\text{catalyst}] = 0.15 \text{ g/L}$ , and initial  $\text{pH} = 6.9$ ).

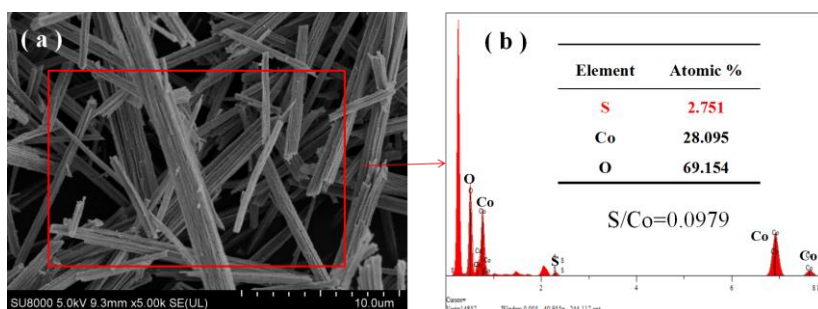


Fig. S9 SEM-EDS images of used  $\text{S-Co}_3\text{O}_4\text{-450}$ .

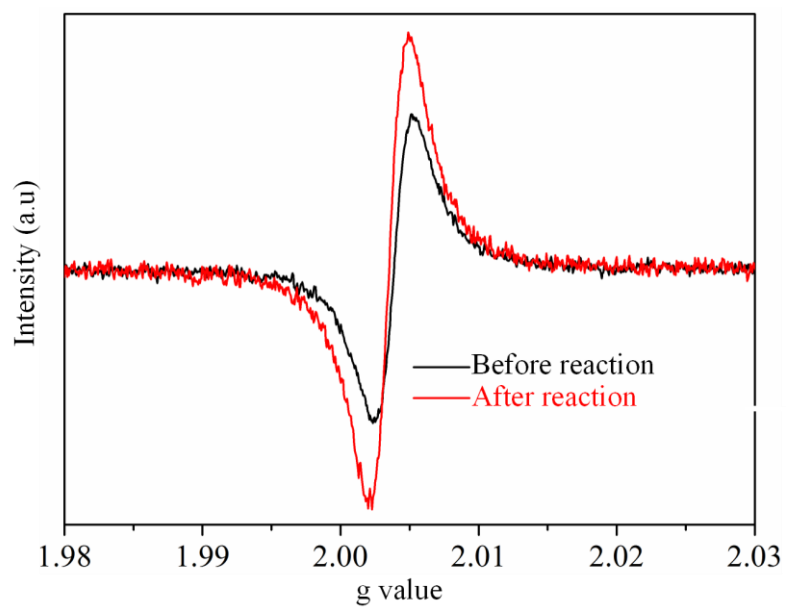


Fig. S10 EPR spectra of S-Co<sub>3</sub>O<sub>4</sub>-450 before and after reaction.

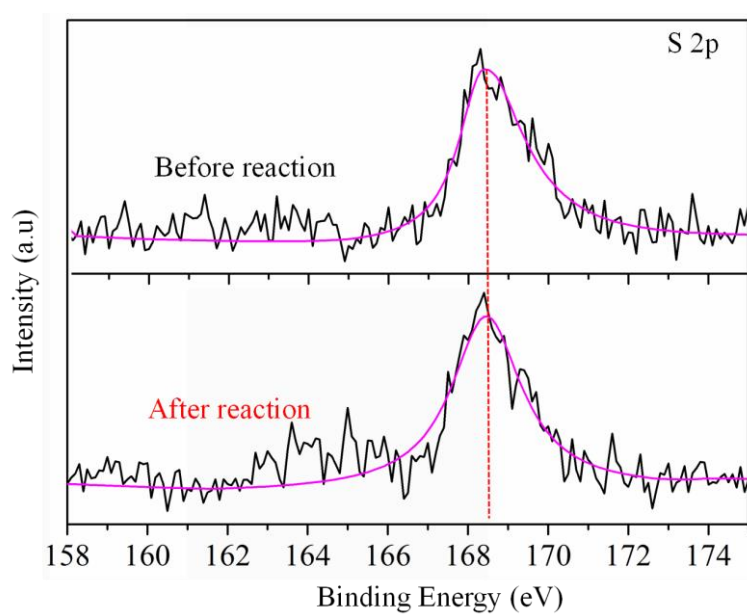


Fig. S11 Fine XPS spectrum of S 2p for S-Co<sub>3</sub>O<sub>4</sub>-450 before and after reaction.

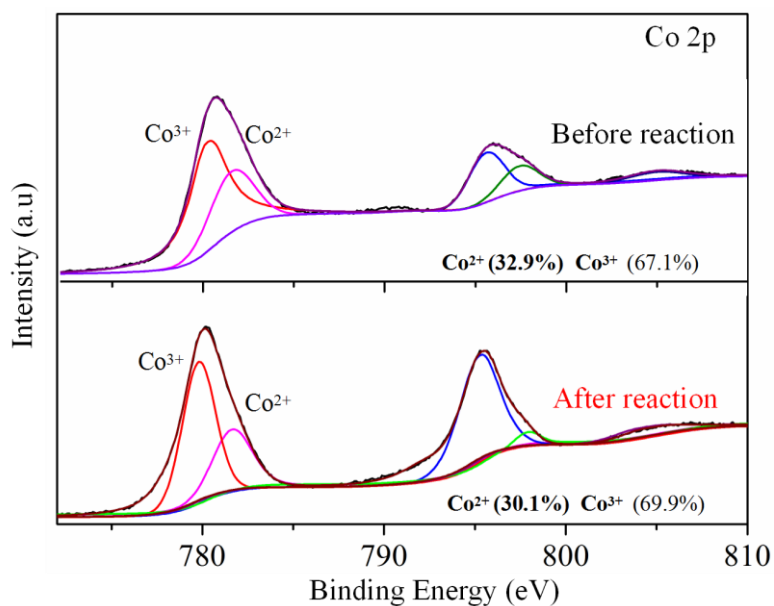


Fig. S12 Fine XPS spectrum of Co 2p for S-Co<sub>3</sub>O<sub>4</sub>-450 before and after reaction.

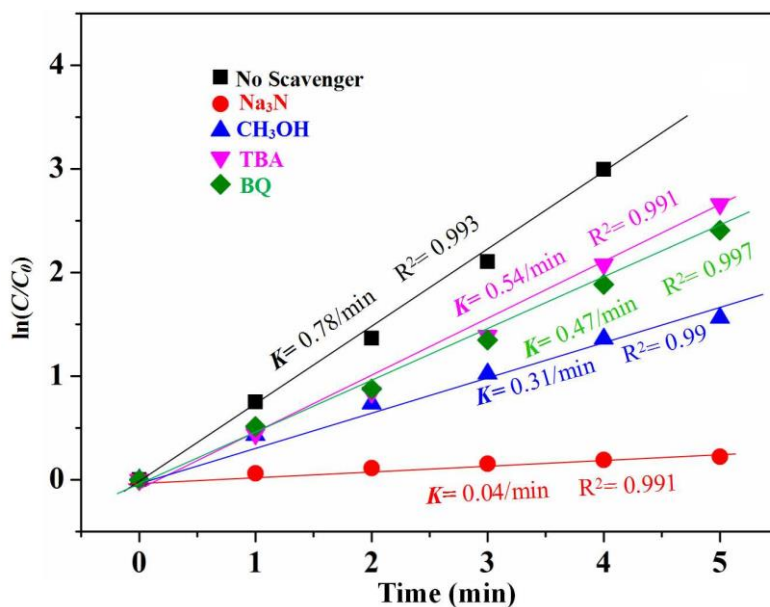


Fig. S13 The quenching effect of different scavengers on the kinetics of MB degradation in S-Co<sub>3</sub>O<sub>4</sub>-450+PMS system ([MB] = 20 mg/L, [PMS] = 0.1 g/L, [S-Co<sub>3</sub>O<sub>4</sub>-450] = 0.15 g/L, T = 25 °C, and initial pH = 6.9)



**Table S1** Structure properties of  $\text{Co}_3\text{O}_4$  and S- $\text{Co}_3\text{O}_4$

Sam.	$A_{\text{BET}}$ ( $\text{m}^2/\text{g}$ )	$d_p$ (nm)
$\text{Co}_3\text{O}_4$ -450	$7.86 \pm 0.08$	41
S- $\text{Co}_3\text{O}_4$ -350	$29.62 \pm 0.03$	13.0
S- $\text{Co}_3\text{O}_4$ -400	$43.33 \pm 0.46$	12.3
S- $\text{Co}_3\text{O}_4$ -450	$58.57 \pm 0.16$	11.1
S- $\text{Co}_3\text{O}_4$ -500	$58.95 \pm 0.23$	11.1

$A_{\text{BET}}$ : specific surface area;  $d_p$ : pore diameter.